Development 138, 1595-1605 (2011) doi:10.1242/dev.052787

The *Drosophila* L1CAM homolog Neuroglian signals through distinct pathways to control different aspects of mushroom body axon development

Tim Goossens[1,2,*], Yuan Y. Kang[3,4,*], Gunther Wuytens[2,5], Pascale Zimmermann[2,5], Zsuzsanna Callaerts-Végh[6], Giulia Pollarolo[2,7], Rafique Islam[8], Michael Hortsch[8] and Patrick Callaerts[1,2,†]

SUMMARY

The spatiotemporal integration of adhesion and signaling during neuritogenesis is an important prerequisite for the establishment of neuronal networks in the developing brain. In this study, we describe the role of the L1-type CAM Neuroglian protein (NRG) in different steps of *Drosophila* mushroom body (MB) neuron axonogenesis. Selective axon bundling in the peduncle requires both the extracellular and the intracellular domain of NRG. We uncover a novel role for the ZO-1 homolog Polychaetoid (PYD) in axon branching and in sister branch outgrowth and guidance downstream of the neuron-specific isoform NRG-180. Furthermore, genetic analyses show that the role of NRG in different aspects of MB axonal development not only involves PYD, but also TRIO, SEMA-1A and RAC1.

KEY WORDS: Neuroglian, Signaling, Mushroom bodies

INTRODUCTION

The formation of neuronal networks during brain development involves fasciculation and defasciculation of axons, integration of signaling to direct growth cones, and control of axonal bifurcation and directed outgrowth of sister branches to establish precise neuronal connections involving multiple targets. It is currently not well understood how extracellular cues and adhesive interactions are integrated spatiotemporally to control neuron subtype-specific neuritogenesis. We study this problem and its mechanistic basis in *Drosophila* mushroom bodies (MBs).

The MBs are prominent neuropils in the central brain of *Drosophila* that are important for different behaviors, including olfactory learning and memory, visual context generalization and courtship conditioning (Liu et al., 1999; Mehren et al., 2004; Davis, 2005). The intrinsic MB neurons, called Kenyon cells, are positioned at the posterior-dorsal cortex, send their dendrites anteriorly into the calyx and project their axons into the peduncle, where fibers fasciculate and project anteroventrally to the heel region (see Fig. 1A). There, larval γ neurons branch into a dorsal and a medial lobe, which are reorganized during metamorphosis to give rise to a single horizontal lobe in the adult MBs. α′β′ neurons, which are formed in late third instar larval stages, and αβ neurons, which arise during puparium formation, project axons that bifurcate and give rise to horizontal β′ and β lobes and vertical α′ and α lobes (Lee et al., 1999). Thus, the establishment of MBs covers a range of axonal development processes, such as outgrowth, branching and guidance.

One family of evolutionarily conserved cell-adhesion molecules comprises the L1-type cell adhesion molecules (L1-type CAMs). Vertebrates have four L1-CAM members (L1, CHL1, Neurofascin and Nr-CAM) (Hortsch, 2000), whereas *Drosophila* has only one, Neuroglian (NRG) (Bieber et al., 1989). L1-deficiency in human and mouse leads to phenotypes that include corpus callosum agenesis, mental retardation, adducted thumbs, spastic paraplegia and hydrocephalus (Fransen et al., 1995; Dahme et al., 1997; Fransen et al., 1998; Demyanenko et al., 1999; Maness and Schachner, 2007). Although considerable insight has been gained in L1-type CAM function, important challenges remain. Specifically, it is not understood how L1-type CAMs act in different molecular complexes or how they integrate various signals to control neuritogenesis.

In this paper, we identify *central brain deranged* alleles as mutations in the *Neuroglian* locus and thereby reveal a role for NRG in different steps of MB development, including fasciculation, axon outgrowth, branching and guidance. Characterization of the mutant alleles shows that the phenotypes are caused by defective cell-cell adhesion and by impaired NRG-initiated signaling. By means of transgenic rescue experiments we identify an important role for the C terminus of the neuronal specific isoform of Neuroglian (NRG-180) in axon branching and sister branch guidance and growth. We show that NRG acts upstream and interacts directly with the MAGUK Polychaetoid (PYD), revealing a novel role for a MAGUK protein during axonal differentiation. In addition, we uncover a genetic network that, apart from *Nrg* and *pyd*, includes *Sema-1a*, *trio* and *Rac1* and that controls distinct aspects of MB development.

MATERIALS AND METHODS

Fly stocks

All stocks were grown on standard medium. Nrg^{1}, Nrg^{2} and Nrg^{3} have been reported previously (Bieber et al., 1989; Hall and Bieber, 1997). The following stocks were generously provided to us: ceb^{849} (Nrg^{849}) and ceb^{892}

[1]VIB, Laboratory of Developmental Genetics, 3000 Leuven, Belgium. [2]Department of Human Genetics, Katholieke Universiteit Leuven, 3000 Leuven, Belgium. [3]Department of Biology and Biochemistry, University of Houston, Houston, TX 77204-5001, USA. [4]Department of Cell Biology, Baylor College of Medicine, Houston, TX 77030, USA. [5]Katholieke Universiteit Leuven, Laboratory for Signal Integration in Cell Fate Decision, 3000 Leuven, Belgium. [6]Katholieke Universiteit Leuven, Laboratory of Biological Psychology, 3000 Leuven, Belgium. [7]VIB, Laboratory of Neuronal Differentiation, 3000 Leuven, Belgium. [8]Department of Cell and Developmental Biology, University of Michigan Medical School, Ann Arbor, MI 48109-2200, USA.

*These authors contributed equally to this work
†Author for correspondence (patrick.callaerts@med.kuleuven.be)

Accepted 24 January 2011

(Nrg^{892}) (M. Heisenberg, Universität Würzburg, Germany); $FRTpyd^{C5}$, $pyd^{EY04259}$, UAS-GFP::PYD (M. Affolter, Universität Basel, Switzerland); pyd^{tam} (J. Schulz, K.U.Leuven, Belgium); $Sema\text{-}1a^{CA07125}$ (A. Spradling, Carnegie Institution, Baltimore, USA); $trio^{M304}$ (B. Dickson, Research Institute of Molecular Pathology, Vienna, Austria); $Rac1^{J11}$, $Rac2^{\Delta}$, Mtl^{Δ} (L. Luo, Stanford University, Stanford, USA); and OK107-GAL4 (S. Sweeney, University of York, UK). A second site mutation on the original Nrg^{892} X chromosome was removed by recombining with an *FRT19A* element (Y. Kang, PhD thesis, University of Houston, 2004). We refer to this allele as FRT,Nrg^{892}. $pyd^{LL04525}$ was obtained from the *Drosophila* Genetic Resource Center (Kyoto, Japan). The *Nrg*-RNAi-line was from the Vienna *Drosophila* RNAi Center (VDRC-6688). Nrg^{G00305} (henceforth referred to as Nrg^{GFP}) (Morin et al., 2001) and other fly stocks were obtained from the Bloomington *Drosophila* stock center (Indiana University, USA). For analysis of MB overexpression of NRG-180 (referred to as OK107>NRG-180), flies with the genotype UAS-NRG-180#30/+; UAS-NRG-180#28b/+;; OK107/+ were used.

Immunohistochemical staining and image analysis

Drosophila brains were dissected, fixed and immunostained as described (Clements et al., 2008). The monoclonal antibodies BP104 (anti-Neuroglian-180, used at 1:10 dilution), 1D4 (anti-Fasciclin 2, 1:100) and 4F3 (anti-Discs Large, 1:20), developed by C. Goodman, and mAbDAC2-3 (anti-Dachshund, 1:20), developed by G. Rubin, were obtained from the Developmental Studies Hybridoma Bank (under the auspices of the NICHD and maintained by The University of Iowa, Department of Biological Sciences, Iowa City, IA 52242). The polyclonal antibody against PYD (anti-Tamou, 1:500) was a gift from R. Ueda (Mitsubishi Kasei Institute of Life Sciences, Japan). For secondary antibodies, FITC-, Cy3- or Cy5-conjugated goat anti-mouse or goat anti-rabbit (Jackson ImmunoResearch Laboratories, USA) were used at a 1:200 dilution. Brains were mounted in Vectashield mounting medium (Vector Laboratories, USA), and analyzed with a Fluoview FV1000 confocal microscope (Olympus). Image processing was carried out with Adobe Photoshop.

Genomic DNA extraction, PCR amplification and sequencing of *Nrg* exons

Genomic DNA was extracted from male flies using standard protocols. Coding sequences of Nrg^{3}, Nrg^{849}, Nrg^{892} and wild-type *Nrg* were PCR amplified with primer pairs situated in *Nrg* intronic sequence (see Table S1 in the supplementary material). PCR products were cloned into pCR-TOPO vector (Invitrogen) and sequenced (for primers, see Table S1 in the supplementary material). Upon initial identification, mutations were confirmed in independent replicate experiments.

Transgenic rescue experiments

The GAL4/UAS system (Brand and Perrimon, 1993) was used to express UAS-NRG-180, UAS-NRG-167 and UAS-NRG::GPI transgenes (Islam et al., 2004) with the OK107-GAL4 driver (Adachi et al., 2003) to rescue mutant *Nrg* MB phenotypes. Progeny were collected at wandering 3rd instar larval stage, and shifted to 29°C until late pupal stage. Hemizygous Nrg^{3} male pharate adults were dissected for antibody staining.

MARCM analyses

For MARCM analysis, Nrg^{1} and *Nrg*-RNAi were used to disrupt NRG function. Nrg^{1} was recombined with *FRT19A* as described previously (Xu and Rubin, 1993). The following genotype was generated to assess *Nrg*-function: Nrg^{1}, *FRT19A*/*FRT19A*, tubP-GAL80, hsFlp; UAS-CD8::GFP/+;; OK107/+ and hsFLP/+; UAS-CD8::GFP/+; FRT2A,UAS-*Nrg*-RNAi/FRT2A,tubP-GAL80; OK107/+. Controls were yw, *FRT19A*/*FRT19A*,tubP-GAL80, hsFlp; UAS-CD8::GFP/+; OK107/+ and hsFLP/+; UAS-CD8::GFP/+; FRT2A/FRT2A,tubP-GAL80; OK107/+. Flies were heat-shocked for 1 hour at 37°C at different developmental stages and allowed to develop to adult stage. Brains were stained with anti-Fasciclin 2 and anti-GFP to analyze the Nrg^{1} clones.

Three-dimensional modeling of *Nrg* mutations

The Hemolin immunoglobulin domain (D1-D4) crystal structure (Su et al., 1998) (PDB accession number 1BIH) was used to model Neuroglian Ig1-Ig4 domains. Alignments between Hemolin D2 and D3 domains and Neuroglian and Human L1-CAM Ig2 and Ig3 domains were based on the published alignment (Sun et al., 1990). Protein structure was visualized with MolMol software (Koradi et al., 1996) (available at www.mol.biol.ethz.ch/groups/wuthrich_group/software).

S2 cell aggregation assay

S2 cells were transfected with inducible $Nrg\text{-}180^{wt}$, $Nrg\text{-}180^{mut849}$ and $Nrg\text{-}180^{mut892}$constructs and cell aggregation assays were carried out as reported previously (Hortsch et al., 1995). *pRmHa-3* $Nrg\text{-}180^{wt}$ containing full-length *Nrg-180* cDNA has been reported before (Hortsch et al., 1995). Nrg^{849} and Nrg^{892} mutations were introduced as follows. An *Eco*RI-*Asp*718 cDNA fragment (~3.8 kb) was excised and cloned into pTOPOXL vector digested with *Eco*RI and *Asp*718. An *Eco*RI-*Acc*I fragment was replaced by a PCR-generated *Eco*RI-*Acc*I fragment containing the Nrg^{849} (C→T) or the Nrg^{892} (G→A) mutations (see Table S1 in the supplementary material for primers). An *Eco*RI fragment of *Nrg-180* was ligated back in the pTOPOXL vector to generate full-length cDNAs, which were cloned into the pRmHa vector as *Asp*718 fragments.

Analysis of genetic interaction

The following alleles of PDZ-domain protein encoding genes were tested for genetic interaction with Nrg: a^{1}, $a^{k11011b}$, a^{7}, a^{EM1}, baz^{EH171}, baz^{4}, baz^{G0484}, cno^{2}, $dlg1^{G0276}$, $dlg1^{G0342}$, $dlg1^{G0456}$, dlt^{04276}, dsh^{1}, dsh^{6}, pyd^{C5}, pyd^{1}, pyd^{tam}, $scrib^{7B3}$, scc^{E8} and $ptpmeg^{EY12179}$. Double mutant flies were analyzed for MB lobe morphology. Interactions of *Nrg*, *pyd*, *trio*, *Rac1* and *Sema-1a* alleles were tested by scoring MB phenotypes in double mutant flies. Statistical analysis was carried out using a two-tailed Fisher's Exact Test, comparing presence and absence of MB phenotypes of double mutants and single Nrg mutants. A two-tailed Fisher's Exact Test was also used to evaluate MB misguidance phenotypes in flies overexpressing NRG-180 and flies in which a mutation was introduced in this overexpression background.

Ligand overlay

PCR primers are listed in Table S1 in the supplementary material. Cytosolic NRG-encoding fragments (NRG-180cyt, NRG-167cyt and NRG-180cyt ΔTYV) were PCR-amplified with full-length *Nrg-180* and *Nrg-167* cDNAs as templates, and *Eco*RI/*Xho*I cloned in the pGEX-5x-3 vector (Amersham Pharmacia). cDNA for the PYD constructs was generated with the Gene Amplifier PCR kit (Perkin Elmer). The fragments encoding PYD-PDZ-domains PDZ1, PDZ2 and PDZ1-2 were generated by PCR on larval cDNA and cloned into the pGEM-T-vector (Promega). The fragments were isolated from the pGEM-T-vector (*Bam*HI/*Not*I for PDZ1 and *Bam*HI/*Eco*RI for PDZ2 and PDZ1-2) and ligated into the pGEXmyc-vector (Grootjans et al., 2000). Full-length PYD-F was created by inserting a *Bgl*II-*Xho*I fragment from clone LP05923 3′ into the pGEM-T- PDZ1-2 vector. This construct was used as template to PCR-amplify PDZ3 and PDZ1-2-3. These fragments were *Bam*HI/*Eco*RI digested and cloned into the pGEXmyc-vector. Production and purification of the GST-fusion proteins, SDS-PAGE and ligand overlay was carried out as described previously (Grootjans et al., 2000).

RESULTS

Central brain deranged alleles are mutations in the *Neuroglian* gene and uncover a role in consecutive steps of MB development

In a genetic analysis of *Neuroglian* (*Nrg*), we tested for allelism with *central brain deranged* (*ceb*) (Strauss and Heisenberg, 1993), which maps to the same cytological position (7F2-F4). *Nrg* (Nrg^{1}, Nrg^{2} and Nrg^{3}) and *ceb* (ceb^{849} and ceb^{892}) alleles failed to complement (results not shown). Subsequently, in ceb^{849} and ceb^{892} flies, we identified mutations in the *Nrg*-coding sequence (see below). Therefore, we refer to ceb^{849} and ceb^{892} as Nrg^{849} and Nrg^{892}

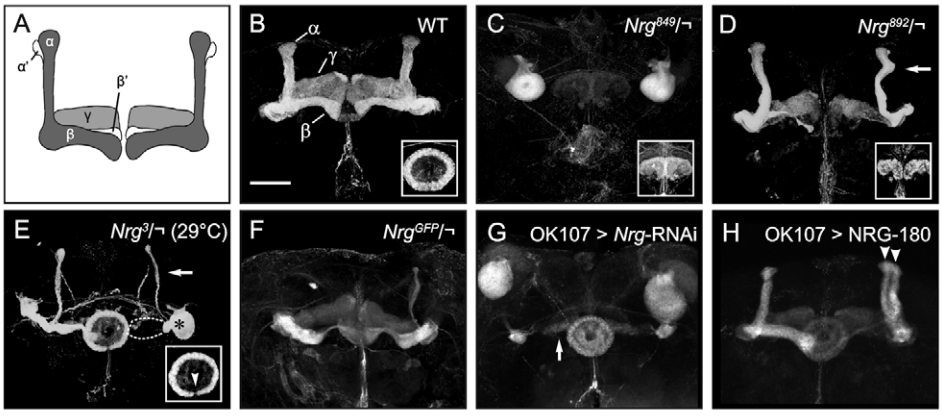

I

		Nrg 849	FRT,Nrg 892	Nrg 3 (a)	Nrg GFP	OK107 > Nrg-RNAi	OK107 > NRG-180
	n (b)	94	84	45	75	19	26
adult γ	thinner	100	14	84	13	100	0
αβ	axon stalling	94	6	90 (c)	7	100	0
	lobe missing (d)	6	45	10	44	0	35
	abnormal morphology (e)	0	51	10	25	0	35
	n (b)	47	41	22	38	10	13
EB	EB VO	0	7	68	50	0	0
	EB split	100	83	14	8	0	0

Fig. 1. Neuroglian mutant phenotypes. Whole-mount anti-FAS2 staining of adult central brain labels EB and α, β and γ MB lobes (see B). All images are projections of confocal z-stacks. Scale bar: 50 μm. (**A**) Schematic representation of *Drosophila* MBs with α, α′, β, β′ and γ lobes. (**B**) Wild-type MB lobes and EB (inset). (**C**) MB axon stalling and a split EB (inset) in hemizygous Nrg^{849}. Only the axon stalling and EB defects are shown in this confocal stack. Gamma lobe phenotypes are the same as in G (see below). (**D**) Nrg^{892} hemizygote with β lobe missing MB phenotype, thinner γ lobes, abnormal α-lobe morphology (arrow) and split EB phenotype (inset). (**E**) MB and EB defects in hemizygous Nrg^{3} grown at restrictive temperature (29°C). MB phenotypes include thinner (arrow) or missing (dashed line) lobes and axon stalling (asterisk). The EB has a ventral open phenotype (arrowhead). (**F**) Nrg^{GFP} hemizygote with thin or missing α lobes, β lobes with outgrowth defects and thinner γ lobes. (**G**) MBs from OK107>*Nrg*-RNAi with axon stalling defects, and a prominent γ lobe defect with thin, often abnormally oriented, lobes (arrow). The EB is wild type, as OK107-GAL4 does not drive expression in this neuropil. (**H**) Lobes of NRG-180 overexpressing MBs show guidance defects (right brain hemisphere): the majority of β axons project vertically, parallel to the α lobe, resulting in two vertical lobes (arrowheads). (**I**) Mushroom body phenotype summary. (a) At 29°C from first instar larval stage until dissection as pharate adults. (b) *n* for MB phenotypes is the number of brain hemispheres analyzed, while *n* for EB phenotypes is the number of brains analyzed. (c) Complete (all axons) or partial (majority of axons) axon stalling. (d) Lobe missing caused by axon branching and/or axon guidance defects. (e) The defects in MB lobe morphology (referred to as abnormal morphology) for the different genotypes is described in detail in the text.

throughout the manuscript. To investigate the role of *Nrg* in central brain development, we used Nrg^{849}, Nrg^{892}, the temperature-sensitive Nrg^{3} [a functional null mutant at the restrictive temperature of 29°C (Hall and Bieber, 1997)], the hypomorphic Nrg^{GFP} line, which has a GFP exon inserted before the last exon of the two *Nrg* isoforms (Morin et al., 2001; Yamamoto et al., 2006), Nrg^{1}, a homozygous lethal null allele (Bieber et al., 1989; Hall and Bieber, 1997), and a *Nrg* RNAi-line (see Fig. S1 in the supplementary material).

We determined central brain defects associated with mutations in *Nrg* using anti-Fasciclin 2 immunohistochemistry, labeling the MB α, β and γ lobes and the ellipsoid body (EB) (Fig. 1A,B), anti-Discs Large 1, to stain all brain neuropils, and OK107-GAL4-driven CD8::GFP, which labels all intrinsic MB neurons.

In third instar larvae, no *Nrg*-associated phenotypes were detected. By contrast, distinct phenotypes were seen in adult brains (Fig. 1). In all mutants, α′β′ axons displayed the same defects as the αβ axons (see below), while the γ lobes were thinner. As the temperature-sensitive Nrg^{3} mutants do not eclose when shifted to restrictive temperature (29°C) during first larval instar, brains were dissected from pharate adults.

The morphology of the αβ lobes was examined in detail. In Nrg^{849} homozygous females and hemizygous males, MB αβ axons mostly grow into ball-like structures around the peduncle region instead of projecting into peduncles and then dorsally and laterally into the lobes (Fig. 1C). This phenotype has been termed axon arrest or axon stalling (Ng et al., 2002). Occasionally, milder αβ lobe defects were observed, such as one lobe (dorsal or lateral) missing. This phenotype is probably due to defects in axon branching and/or axon guidance. The latter is characterized by α axons growing along the β lobe or β axons growing along the α lobe, instead of projecting to their normal target area. FRT,Nrg^{892} flies show less severe phenotypes, including missing or misguided lobes as well as full-length MB lobes that do not grow straight vertically or medially (Fig. 1D). The temperature-sensitive Nrg^{3} mutants revealed strong MB phenotypes, with complete or partial αβ axon stalling, and milder phenotypes such as thinner or missing lobes (Fig. 1E). Nrg^{GFP} flies displayed thinner or missing αβ lobes, as well as abnormalities of lobe morphology, mainly owing to partial β outgrowth defects (Fig. 1F). RNAi downregulation of *Nrg* in all intrinsic MB cells with OK107-GAL4 (see Fig. S1 in the supplementary material) resulted

in all MBs displaying an αβ axon stalling phenotype (Fig. 1G), comparable with Nrg^{849}. To assess whether the strong phenotypes in Nrg^{849} hemizygotes and *Nrg*-RNAi expressing flies, including the thinner γ lobes, are (partially) due to a reduction in mushroom body cell number, we counted the number of dorsal posterior cortex nuclei that are immunopositive for Dachshund (DAC), a nuclear protein expressed in Kenyon cells (Kurusu et al., 2000; Martini et al., 2000; Noveen et al., 2000). We found that the number of DAC-positive cells in these mutants was not reduced compared with control flies (see Fig. S2 in the supplementary material).

When we overexpressed the neuron-specific NRG-180 isoform using OK107-GAL4, we observed defects in MB lobe morphology. These include phenotypes caused by defects in guidance (e.g. two lobes running parallel as seen in Fig. 1H) and fasciculation (see Fig. S3 in the supplementary material).

Nrg mutants also display EB phenotypes. In Nrg^{3} and Nrg^{GFP} flies, we mainly observed a 'ventral open' defect (Fig. 1E), while the majority of *FRT*,Nrg^{892} and Nrg^{849} mutants show a 'split' phenotype (Fig. 1C,D).

Neuroglian function is essential for axonogenesis during late larval and early pupal stages

To define the role of NRG signaling in MB axonal development, we first determined the spatiotemporal requirements for NRG. We analyzed the distribution of Neuroglian-180 protein using the BP104 antibody (for antibody specificity see Fig. S1 in the supplementary material). NRG-180 is expressed throughout the brain at all stages (Fig. 2A,B). The staining is prominent in axons (Fig. 2A-D″), but cell bodies also reveal distinct labeling (Fig. 2E-E″). In larval, pupal and adult MB neurons NRG-180 expression is detected in all lobes. Adult MBs display a high expression level in the γ and αβ lobes, while expression is lower in the axons of the α′β′ neurons (Fig. 2C-D″).

The quantitative and qualitative differences between phenotypes seen in γ axons and the later-born α′β′ and αβ neurons (see Fig. 1) may reflect a differential NRG requirement in distinct MB neuronal subtypes. We tested this in temperature shift experiments with the temperature-sensitive allele Nrg^{3} in the presence of OK107-GAL4 driven GFP::CD8 to label all MB neurons (Fig. 3). No MB phenotypes were observed in third instar larvae that were shifted to 29°C from first instar larval stage (Fig. 3B). Neither did we find penetrant MB defects in adult brains of flies raised at 29°C from first until late third larval instar and at 18°C for the rest of development (Fig. 3C). When raised at 29°C between late third instar larval stage and 24 hours APF (after puparium formation), Nrg^{3} flies exhibited strong and penetrant MB defects (Fig. 3D), resembling the phenotypes seen in the Nrg^{849} and OK107>*Nrg*-RNAi mutants (Fig. 1). No obvious phenotypes were seen in Nrg^{3} mutant animals when shifted to the restrictive temperature 24 hours APF (Fig. 3E).

In summary, NRG is crucial during late larval and early pupal stages for MB development.

NRG is cell-autonomously required for axonogenesis in a subset of MB neurons

The phenotypes associated with *Nrg* mutations suggest that *Nrg* regulates different aspects of axon development. To determine which of these processes require *Nrg* and to investigate whether NRG is required cell autonomously in MB neurons, we used mosaic analysis with a repressible cell marker (MARCM) (Lee and Luo, 1999).

We analyzed neuroblast clones that expressed *Nrg*-RNAi or that were homozygous for Nrg^{1}, a previously identified protein null allele (Bieber et al., 1989). Both functional disruptions resulted in similar neuroanatomical abnormalities, including MB axon misprojection, β-axon overextension and branching defects, with axons failing to bifurcate into horizontal and vertical lobes (Fig. 4B; data not shown).

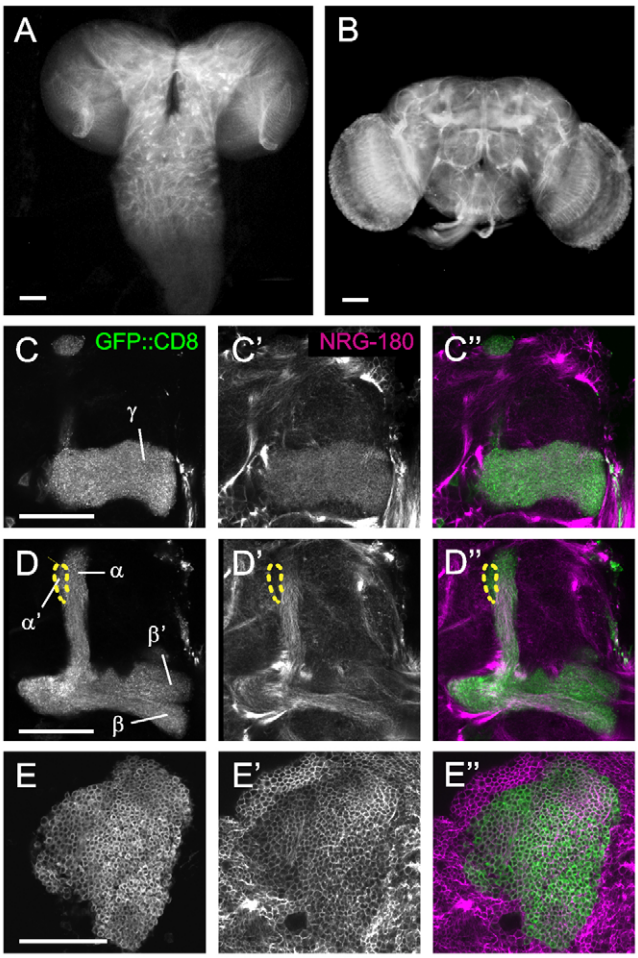

Fig. 2. Neuroglian expression in the postembryonic brain. (**A**,**B**) NRG-180 is broadly expressed in the *Drosophila* brain at 3rd instar larval (A) and adult (B) stages. (**C-E″**) Single confocal sections of anti-NRG-180 staining (C′-E′) on flies expressing CD8::GFP under control of the OK107-GAL4 driver to mark the MB neurons (C-E; C″-E″ shows merged pictures). NRG-180 staining is readily observed in the γ axons (C-C″) and the αβ axons (D-D″), while α′β′ lobe expression is lower (D-D″). NRG-180 levels are often observed to be lower in the α, β, α′ and β′ lobe tips. The broken lines in D-D″ show the outline of the α″ lobe tip, in which NRG-180 can hardly be observed. (E-E″) NRG-180 is also localized in the cell bodies of the Kenyon cells. Scale bars: 50 μm.

We then investigated mutant Nrg^{1} single cell clones in detail, to assess the cell-autonomous roles of *Nrg*. The most frequently observed phenotypes were defects in axon branching (Fig. 4D) and outgrowth (Fig. 4E). Because the distinction between α/β branching defects and putative outgrowth defects with a minimal α or β sister branch could not always reliably be made, they were grouped together (summarized in Fig. 4G). Defects were mainly found in mutant αβ cells induced at prepupal stages. In these cells, axon branching and outgrowth defects were observed in 23% of cases. To a lesser extent, defects were also found in clones induced at other developmental stages (Fig. 4G). In a fraction of clones, we observed Kenyon cell bodies without axonal/dendritic outgrowth.

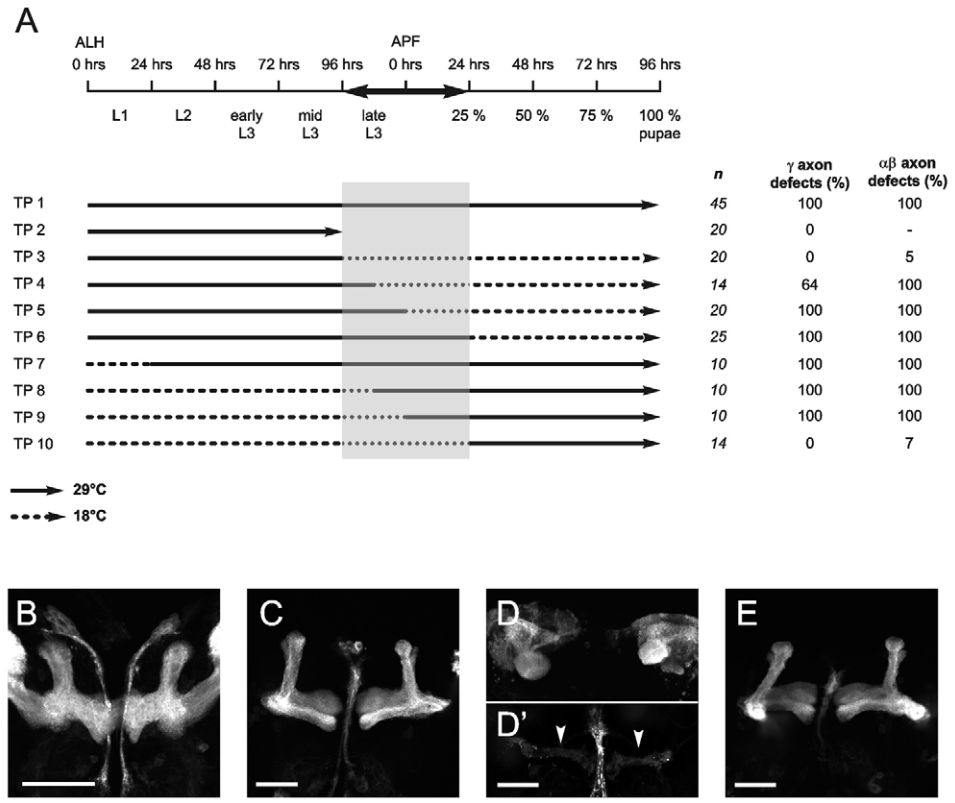

Fig. 3. Neuroglian function is necessary during late larval and early pupal stages. (**A**) Diagram of different temperature shifts. The timeline at the top refers to developmental time at 25°C. Wild-type (WT) and *Nrg*^{3} embryos were collected at 18°C. First instar larvae were collected within 3 hours of larval hatching (ALH), and then exposed to different temperature programs (TPs 1-10). Broken lines indicate incubation at 18°C (permissive temperature). Black lines represent incubation at 29°C (restrictive temperature). The arrows indicate the time of dissection. αβ and γ lobe phenotypes were scored in anti-FAS2 stained brains. Penetrant neuroanatomical MB defects were found in flies raised at 29°C between late third instar larval (L3) stage and 24 hours after puparium formation (APF). *n* is the number of brain hemispheres analyzed. (**B-E**) MBs from *Nrg*^{3}/–; UAS-GFP::CD8/+;; OK107/+ flies, subjected to one of the TPs depicted in A. (B) MBs from TP 2 larvae are normal. (C) MBs from TP 3 flies do not display mutant phenotypes. (D-D′) Strong MB phenotypes are observed in TP 5 flies. D shows αβ axon stalling phenotypes. D′ displays thin γ neurons (arrowheads; same brain as in D, but image taken at higher high voltage confocal settings). (E) MBs from TP 10 flies do not show mutant phenotypes.

Although this phenotype was only rarely seen in wild-type clones (2.5%), it occurred at much higher frequency in *Nrg*^{1} clones (11.5%). Occasionally, *Nrg*^{1} mutant cells displayed other phenotypes, such as local MB lobe defasciculation (1.6%) and axonal misprojection to other brain regions (2.2%) (Fig. 4F). These phenotypes were never observed in wild-type control clones.

In summary, these data infer a time-specific and cell-autonomous component of NRG signaling in MB-development, with NRG being involved in multiple steps of axon projection, including fasciculation, outgrowth, branching as well as guidance.

Molecular characterization of mutant alleles reveals cell adhesion-dependent and -independent roles for Neuroglian during MB development

To analyze the molecular mechanism of Neuroglian function, we molecularly characterized three *Nrg* alleles. In *Nrg*^{3}, two missense mutations were uncovered at position 735 (G→A) and at position 752 (G→A) of exon 4, resulting in G313D and V319M amino acid substitutions. These mutations were characterized by Kang (Y. Kang, PhD thesis, University of Houston, 2004) and identified independently by Yamamoto et al. (Yamamoto et al., 2006). *Nrg*^{849} has a C→T transition at position 435 in exon 4, resulting in a S213L substitution, while *Nrg*^{892} has a G→A transition at position 404 in exon 4, causing a D203N substitution. We then determined the effects of these mutations on protein structure and function. We first modeled the mutations (Fig. 5A). G313D and V319M (*Nrg*^{3}), reside in the core of the Ig3 domain, and are likely to affect protein folding and consequently protein transport leading to accumulation in the cell body (see also Hall and Bieber, 1997). S213L (*Nrg*^{849}) is situated on the Ig2 domain surface where it may influence protein conformation and/or protein-protein interaction. D203N (*Nrg*^{892}) is conserved between *Drosophila* Neuroglian and human L1-CAM, as well as in the Hemolin D2 domain. It is also on the surface of the Ig2 domain, and the substitution might affect protein conformation and protein-protein interaction.

We directly analyzed whether the *Nrg*^{849} and *Nrg*^{892} substitutions interfere with homophilic interaction using cell culture-based aggregation assays. NRG-180, when transfected in S2 cells, can mediate homophilic interaction (Hortsch et al., 1998a) (see Fig. 5C,F). The *Nrg*^{849} S213L mutation completely abolished cell aggregation (Fig. 5E,F). This corresponds to the effects on homophilic interaction of a point mutation of the corresponding amino acid in human L1-CAM (H201Q) in an individual with

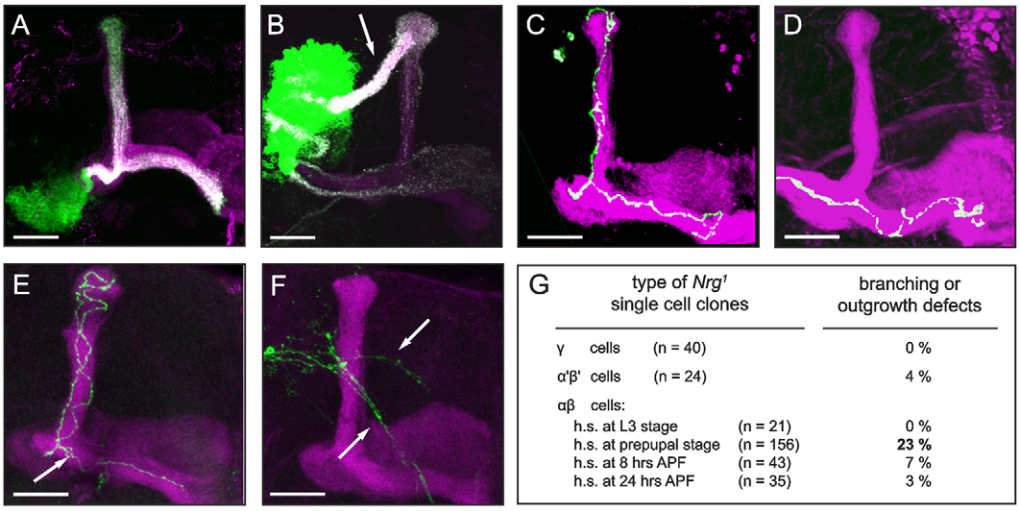

Fig. 4. *Nrg*-RNAi and *Nrg¹* MARCM-clones display defects in axon guidance, branching and outgrowth. (A-F) MBs are visualized with anti-FAS2 (magenta) and homozygous (mutant) cells with anti-GFP (green) (**A**) Wild-type αβ neuroblast clone. (**B**) *Nrg*-RNAi neuroblast clone. Several MB axons display a misprojection phenotype (arrow), bypassing the peduncle and growing directly to the tip of the α lobe. (**C**) Wild-type αβ single cell clone. (D-F) *Nrg¹* mutant αβ clones. (**D**) Branching defect with the neuron failing to form a vertical axon branch. (**E**) Two-cell clone; the horizontal axon branch of one mutant MB neuron does not grow to the tip of the β-lobe, but forms a stubble around the MB-heel region (arrow). (**F**) *Nrg¹* MB neurons misprojecting to other brain regions (arrows). (**G**) Summary of phenotypes observed in *Nrg¹* single cell clones. *n* represents the number of analyzed clones per category. Scale bars: 20 μm.

MASA syndrome (Zhao and Siu, 1996). The Nrg^{892} D203N mutation has no effect on homophilic interaction, as transfected cells can form aggregates (Fig. 5D,F) not significantly different from those mediated by wild type NRG-180 (Fig. 5C,F). Nevertheless, the identification in an individual with MASA syndrome of a similar point mutation (D202Y) indicates that the conserved amino acid is functionally important (Sztriha et al., 2000).

In summary, the strong phenotypes in Nrg^{849} and Nrg^{3} appear to be caused by defective axonal NRG-homophilic interaction or a diminished transport of the mutant protein to the cell surface, respectively. The milder phenotype in Nrg^{892} mutant brains is probably caused by the disruption of other extracellular domain-mediated interactions.

Transgenic rescue provides evidence for separable, isoform-specific roles of Neuroglian in axon fasciculation and branching

Our molecular analysis suggests that the observed phenotypes may be caused by defects in homophilic adhesion or other properties mediated by the extracellular or cytoplasmic parts of the Neuroglian protein. It has previously been demonstrated that ELAV-dependent alternative splicing generates two Neuroglian protein isoforms in *Drosophila*. NRG-167 is ubiquitously expressed and non-neuron specific, whereas NRG-180 is neuron specific (Koushika et al., 1996). Both isoforms share the same extracellular domains, transmembrane domain and part of the cytoplasmic domain containing a conserved ankyrin binding site (see Fig. 6A for schematic representation). We performed rescue experiments of Nrg^{3} MB phenotypes with different transgenes to determine whether both NRG isoforms are functionally equivalent.

Hemizygous Nrg^{3} males and hemizygous Nrg^{3} males also heterozygous for OK107-GAL4, UAS-*Nrg-167* or UAS-*Nrg-180* display the same MB phenotype. Only a fraction of αβ-axons project to the peduncle, while the majority stalls close to the Kenyon cell bodies (Fig. 6C,F).

NRG-167 expression in a Nrg^{3} mutant background, using OK107-GAL4, partially rescues this phenotype. In 92% of analyzed brain hemispheres, αβ-neuron peduncles were observed (Fig. 6D). However, only 21% of α and β lobes displayed a full-length lobe phenotype. Similar results were obtained in Nrg^{3} hemizygous flies containing 2 UAS-*Nrg-167*-constructs driven by OK107-GAL4 (100% with peduncle, 8% with full-length α/β lobes) (Fig. 6F).

By contrast, expression of NRG-180 almost fully rescues the mutant phenotype; 94% of analyzed brain hemispheres have peduncles and full-length αβ lobes (Fig. 6E,F). Similar results were obtained with three different UAS-*Nrg-180* lines. The extracellular domain alone is insufficient as expression of NRG-GPI does not rescue the phenotype (data not shown). All these data suggest that NRG-180 is necessary in MB neurons for normal axon projection, and that its specific cytoplasmic region is required in this process.

The MAGUK protein Polychaetoid acts downstream of NRG-180 in MB development

The rescue experiments indicate that NRG-180-specific signaling is important for MB development. The NRG-specific C terminus has an additional 63 amino acids compared with NRG-167 and contains a putative PDZ-interacting domain. Therefore, we hypothesized that NRG-180 interacts with a PDZ-domain containing protein. To identify this interaction partner, we scored MB α and β lobe phenotypes in heterozygous and hemizygous Nrg^{GFP} flies and heterozygous Nrg^{849} flies that were also heterozygous for a mutation in PDZ-protein-coding genes. Only for one gene, *pyd*, did all the tested hypomorphic alleles (pyd^{C5}, pyd^{1}, pyd^{tam}) display a prominent genetic interaction with the *Nrg*-alleles. Moreover, in NRG-180-overexpressing MBs, misguidance phenotypes were suppressed when a *pyd* mutation was introduced (see Fig. 7 and see Table S2 in the supplementary material), consistent with PYD acting downstream of NRG-180. OK107-

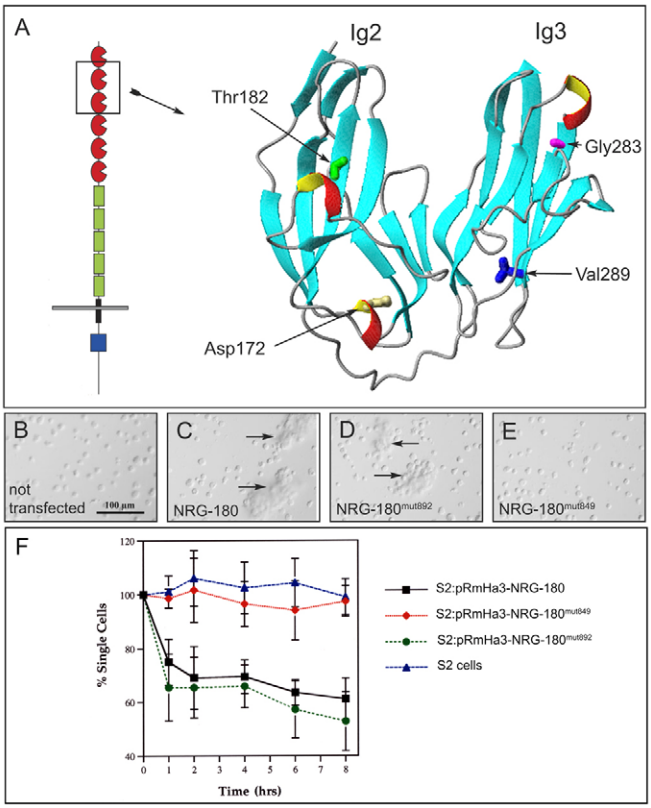

Fig. 5. Mutation analysis of *Nrg*^{849}, *Nrg*^{892} and *Nrg*^{3}. (**A**) Model of Ig2 and Ig3 domains of Neuroglian, using the crystal structure of D2 and D3 domains of Hemolin. The affected amino acids in the Neuroglian mutants are colored: Asp203Asn in NRG^{892} (Asp172 in Hemolin, yellow); Ser213Leu in NRG^{849} (Thr182 in Hemolin, green); Gly313Asp in NRG^{3} (Gly283 in Hemolin, magenta) and Val319Met in NRG^{3} (as Val289 in Hemolin, blue). (**B-E**) S2 cell aggregation assay. S2 cells stably transfected with *Nrg-180*^{wt} cDNA (C) or *Nrg-180*^{mut892} cDNA (D) form aggregates (arrows), whereas untransfected cells (B) and *Nrg-180*^{mut849}-transfected cells (E) do not. (**F**) Graph representing aggregation of *Nrg*-transfected and -untransfected S2 cells. The aggregation of *Nrg-180*^{wt}- and *Nrg-180*^{mut892}-transfected S2 cells results in a decrease of the percentage of single cells over time. No such decrease was observed for cells transfected with *Nrg-180*^{mut849} or for the untransfected control.

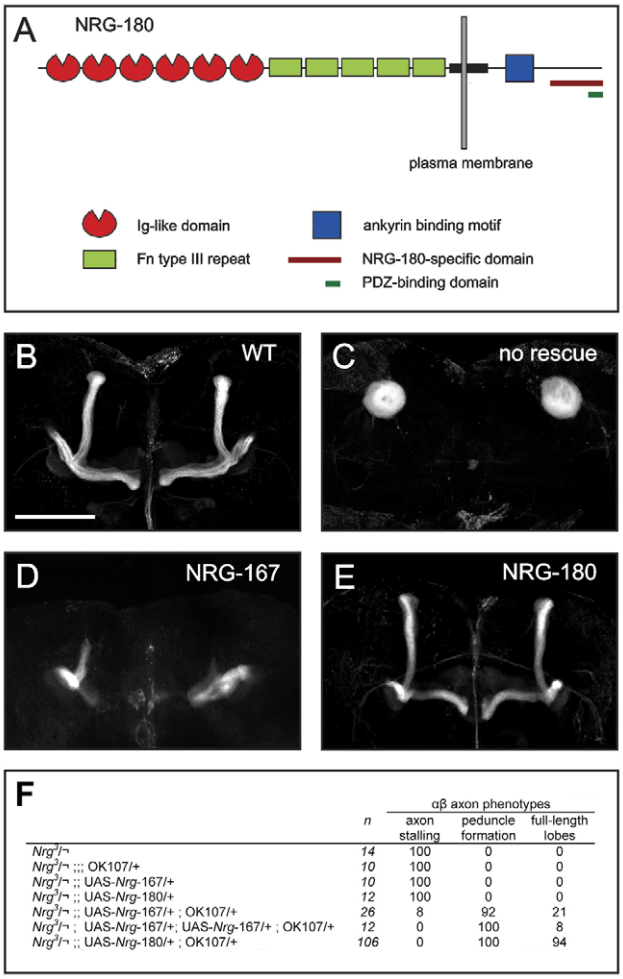

F

	n	αβ axon phenotypes: axon stalling	peduncle formation	full-length lobes
Nrg^{3}/¬	*14*	100	0	0
Nrg^{3}/¬ ;;; OK107/+	*10*	100	0	0
Nrg^{3}/¬ ;; UAS-*Nrg*-167/+	*10*	100	0	0
Nrg^{3}/¬ ;; UAS-*Nrg*-180/+	*12*	100	0	0
Nrg^{3}/¬ ;; UAS-*Nrg*-167/+ ; OK107/+	*26*	8	92	21
Nrg^{3}/¬ ; UAS-*Nrg*-167/+; UAS-*Nrg*-167/+ ; OK107/+	*12*	0	100	8
Nrg^{3}/¬ ;; UAS-*Nrg*-180/+ ; OK107/+	*106*	0	100	94

Fig. 6. Phenotypic rescue of MB defects by transgenic expression of NRG-180, but not NRG-167. (**A**) Scheme of NRG-180 protein structure. (**B-E**) Anti-Fasciclin 2 (1D4) staining of pharate adult brains. (B) *yw* control with normal MB morphology. Scale bar: 50 µm. (C) *Nrg*^{3}/–;;; OK107/+ with αβ axon stalling phenotype (γ lobes not shown). (D) Rescue of peduncle formation and partial rescue of lobe structure in *Nrg*^{3}/–;; UAS*Nrg-167*/+; OK107/+ brains. (E) Full rescue in *Nrg*^{3}/–; UAS*Nrg-180*/+;; OK107/+ displaying wild-type MB morphology. (**F**) Summary of αβ axon phenotypes listing percentages of brains with the relevant phenotype. *n* is the number of brain hemispheres analyzed.

GAL4-driven overexpression of UAS-PYD::GFP (see below) in a *Nrg*^{3} or *Nrg*^{849} mutant background, however, did not result in phenotypical rescue (data not shown).

Homo- or hemizygosity for hypomorphic mutations in *pyd* alone also resulted in MB lobe phenotypes. A short α lobe was found in 7% of *pyd*^{EY04259} brain hemispheres (*n*=14) (Fig. 8A) and in 7% of *pyd*^{EY00825} hemispheres (*n*=30), while thinner α lobes occurred in 38% of *pyd*^{BG02748} hemispheres (*n*=40). In *pyd*^{LL04525} flies, 50% of α and β lobes were thin or missing (Fig. 8C), 20% of β lobes displayed an overextension phenotype, 10% of α lobes was short and in 5% of α lobes, a misguidance defect was observed (Fig. 8D) (*n*=20). In flies hemizygous for *pyd*^{KG02008}, *pyd*^{C5} and *pyd*^{EY04259}, missing lobes were detected in 14% (*n*=22) (Fig. 8B), 5% (*n*=22) and 5% (*n*=22) of brain hemispheres, respectively. We did not observe any obvious defects in the gamma lobes.

Polychaetoid is expressed in Kenyon cells and NRG-180 directly binds to PDZ-domain 1 of PYD

Since the genetic interaction data imply that NRG and PYD are components of a signaling pathway active in MB development, we determined whether NRG and PYD (1) colocalize in the MBs and (2) physically interact. In the late larval and early pupal brain, PYD expression levels were high in the optic lobe proliferation centers and cells in the pars intercerebralis, and lower throughout the rest of the central brain (Fig. 8E; see Fig. S1 in the supplementary material). PYD immunostaining on flies expressing GFP::CD8 with an OK107-GAL4 driver, revealed colocalization of PYD immunoreactivity with GFP on the plasma membrane of the Kenyon cell bodies (Fig. 8F,G). In addition to PYD being detected in Kenyon cell bodies, we also obtained evidence for a putative axonal PYD localization in these cells. In neurons where PYD is

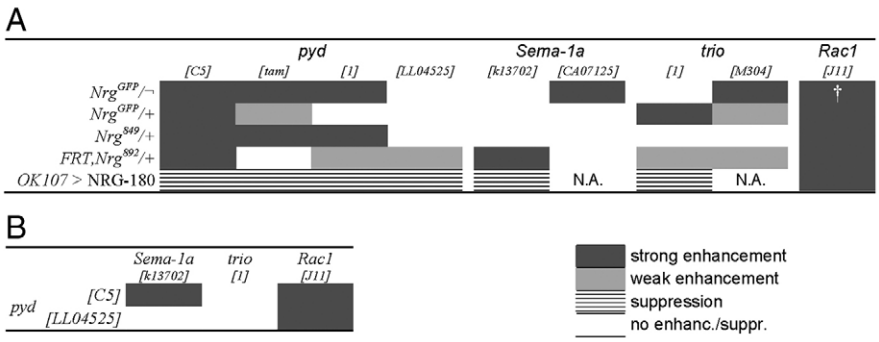

Fig. 7. Summary of genetic interaction experiments. (**A**,**B**) Genetic interactions between *Nrg* and *pyd*, *Sema-1a*, *trio* and *Rac1* (A), and *pyd* and *Sema-1a*, *trio* and *Rac1* alleles (B). Double mutant combinations resulting in an exacerbated MB phenotype are shown in gray. Statistical significance was determined using Fisher's Exact Test (FET). Significantly different allelic combinations ($P<0.03$) are dark gray. Combinations with $P>0.03$, but that displayed (low-penetrant) MB defects while the single mutants had 100% wild-type phenotypes, are light gray. Suppression of the NRG-180 overexpression phenotype, characterized by reduced misguidance phenotypes (FET: $P\leq0.03$) is marked with a horizontally striped pattern. Single heterozygous mutant *pyd, Sema-1a*, *trio* and *Rac1* flies did not display MB phenotypes. See Table S2 in the supplementary material for details.

expressed at higher levels, such as in cells in the pars intercerebralis, PYD can be readily detected in cell bodies, whereas lower protein levels are visible in the axons (see Fig. 8G). In addition, we analyzed the subcellular localization of GFP::PYD, a fusion protein that has a subcellular organization similar to endogenous PYD (Jung et al., 2006). The fusion protein was expressed in larvae and adults with OK107-GAL4, which drives expression in MB cells and pars intercerebralis cells. In both cell types, PYD::GFP was present in cell bodies as well as in axons (Fig. 8G′ and 8G″).

In summary, we showed that NRG and PYD colocalize in Kenyon cells during late larval and early pupal stages, time periods during which NRG is required for MB development.

Finally, to analyze physical interaction of NRG-180 and PYD, we used ligand overlay experiments with the cytosolic parts of NRG-167 (NRG-167cyt), NRG-180 (NRG-180cyt) and NRG-180, which lacks the last three amino acids of the PDZ-interacting domain (NRG-180cytΔTYV) that are predicted to be crucial for PDZ-domain interaction (Hung and Sheng, 2002), and with GST-myc-fusion proteins, which contain one or more of the three PYD-PDZ-domains. NRG-180cyt-binding with myc-tagged PDZ-2, PDZ-3 and the myc-fragment did not exceed background levels, which are caused by GST-GST dimerization (Fig. 8H). However, NRG-180cyt, but not NRG-167cyt or NRG-180cytΔTYV, exhibited an elevated binding affinity for myc-tagged PDZ-1-2-3, PDZ-1-2 and PDZ-1. In summary, the cytoplasmic domain of NRG-180 binds directly to the first PDZ domain of PYD.

Nrg signaling in MB development involves *Rac1*, *trio and Sema-1a*

The transgenic experiments show that peduncle formation depends on the part of the NRG protein shared between NRG-167 and NRG-180, as the axonal stalling phenotype is rescued by both isoforms. Normal lobe morphology, however, requires the additional 63 amino acids present in the NRG180 isoform. For the latter, we have shown that the interaction with PYD is required. The presence of axonal stalling and axon guidance phenotypes stimulated us to identify additional components of the signaling mechanism(s) that involve Nrg by means of genetic experiments and a candidate gene approach.

Axonal stalling phenotypes have previously been seen in mutants of *Rac1*, a member of the Rho family of small GTPases (Ng et al., 2002), and *trio*, a guanine nucleotide exchange factor essential for RAC1 activation (Awasaki et al., 2000; Hakeda-Suzuki et al., 2002). Moreover, the fact that many signal transduction pathways involved in axonal morphogenesis converge on Rho GTPases (Huber et al., 2003) make RAC1 and TRIO plausible downstream effectors of NRG signaling in MB axon development.

The axon guidance phenotypes seen in *Nrg* mutants raise the issue of whether specific axon guidance molecules may be involved. Several lines of evidence suggest that *Sema-1a* (Yu et al., 1998) may be a good candidate. L1-CAM, the vertebrate homolog of NRG, together with Neuropilin and Plexin, mediate axon guidance by forming a receptor complex for secreted SEMA-3A (Castellani et al., 2000; Castellani et al., 2002). In *C. elegans*, the NRG homolog LAD-2 has been found to be involved in Sema2 signaling (Wang et al., 2008), whereas, in *Drosophila*, evidence has been presented that *Nrg* interacts with *Sema-1a* during giant fiber system development (Godenschwege and Murphey, 2009).

We analyzed MB phenotypes in heterozygous and hemizygous Nrg^{GFP} flies and heterozygous Nrg^{849} and FRT,Nrg^{892} flies that were also heterozygous for a mutation in either *Sema-1a*, *Rac1* or *trio*. We observed genetic interaction for each of these genes with at least two *Nrg* alleles (see Fig. 7 and see Table S2 in the supplementary material). Introducing null mutations of two other RacGTPases, *Rac2* and *Mtl*, in an *Nrg* mutant or an *Nrg,Rac1* mutant background did not have any effect on the MB phenotypes (data not shown).

Misguidance phenotypes of NRG-180 overexpressing MBs were suppressed when *Sema-1a* or *trio* mutations were introduced, whereas a mutation in *Rac1* resulted in exacerbated MB defects (see Fig. 7; see Table S2 in the supplementary material).

Finally, we tested for interactions among the four different *Nrg* interactors we identified. We detected strong genetic interaction between the *pyd* and *Rac1* alleles, mainly characterized by axon stalling and guidance defects (see Fig. 7; see Table S2 in the supplementary material). Genetic interaction was also observed between the $Sema\text{-}1a^{k}$ and the pyd^{C5} alleles, with double heterozygotes displaying axonal guidance and overextension defects (see Fig. 7; see Table S2 in the supplementary material).

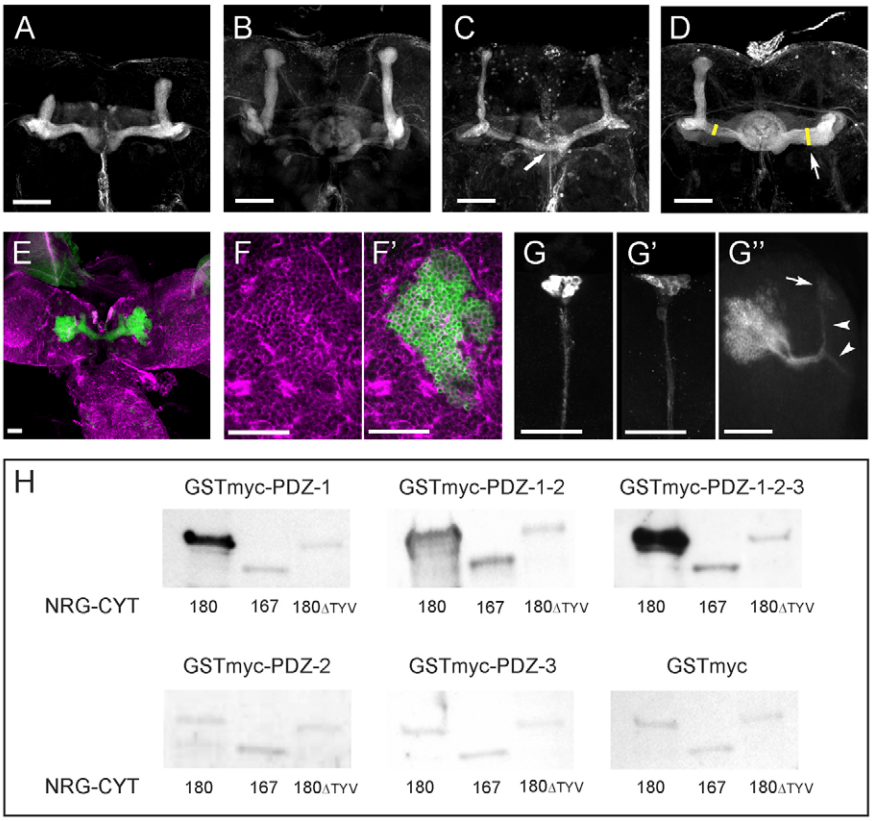

Fig. 8. Polychaetoid localizes to MB neurons and interacts directly with Neuroglian. (A-D) *pyd* mutant MB phenotypes. (**A**) $pyd^{EY04259}$ homozygous mutant with short α lobe. (**B**) MB of $pyd^{KG02008}$/pXT103 fly with malformed β-lobes (pXT103 is a chromosome with a deficiency spanning the *pyd* locus). (**C**,**D**) $pyd^{LL04525}$ mutant MBs with thin lobes and β-lobe fusion (C, arrow) or without a correctly formed α lobe (D). The medial lobe in the right hemisphere is twice as thick as the one in the left hemisphere (see arrow and yellow lines in D), suggestive of α axons being misguided along the β lobe. (**E**) Pupal brain (17 hours after puparium formation) expressing GFP::CD8 (green) under control of the OK107-GAL4 driver and stained with anti-PYD (magenta). PYD is broadly expressed in the ventral ganglion and in the brain hemispheres. (**F**,**F′**) Higher magnification of E, showing the Kenyon cell bodies. Single confocal sections are shown. (**G-G″**) Evidence of axonal localization of PYD. (G) Anti-PYD staining on cells in the pars intercerebralis of an adult brain. PYD is highly expressed in the cell bodies, while a lower expression level can be detected in the axons. (G′,G″) UAS-PYD::GFP under control of the OK107-GAL4 driver results in overexpression of the fusion protein in cells in the pars intercerebralis (G′) and in the MBs (G″, larval MBs). In both cell types, axonal localization of the fusion protein can be observed. PYD::GFP in the MB lobes can only readily be detected in the core, owing to low expression levels. Scale bars: 50 μm. (**H**) Ligand overlay. Protein fragments of the cytosolic parts of NRG-167, NRG-180 and NRG-180 without the three most C-terminal amino acid residues (NRG-180ΔTYV) were purified and blotted on a membrane. The membrane was incubated with GST-myc-fusion proteins, containing one or more of the three PYD-PDZ-domains. Anti-Myc staining shows an elevated binding affinity of the NRG-180 fragment, but not of the NRG-167 and NRG-180ΔTYV fragments, for PYD fragments that contain the first PDZ domain. For loading control, see Fig. S4 in the supplementary material.

DISCUSSION

In the current study, we have demonstrated a requirement for Neuroglian signaling in different steps of mushroom body (MB) axonogenesis, namely (1) axonal projection into the peduncle, and (2) branching, outgrowth and guidance of axonal sister branches. The two steps in mushroom body axonogenesis are genetically separable and seem to involve distinct NRG signaling complexes.

In peduncle formation, NRG signaling does not rely on the NRG-180-specific intracellular domain, but on the extracellular domain and the part of the cytoplasmic domain common to both NRG isoforms. The extracellular domain contributes intercellular adhesive properties, necessary for axon fasciculation into a peduncle. This conclusion is supported by the defective adhesive properties of the NRG^{849} mutant protein in cell aggregation assays, and by the fact that Nrg^{849} hemizygotes frequently lack the peduncle. Interaxonal fasciculation in the peduncle probably involves binding to and stabilization by the actin cytoskeleton network via the ankyrin-binding domain shared by the two NRG isoforms. This conclusion is supported by previous aggregation experiments in *Drosophila* S2 cells in which it was shown that homophilic binding of NRG leads to recruitment of ankyrin to the contact sites (Dubreuil et al., 1996; Hortsch et al., 1998b) and by the observation that RNAi-mediated knockdown of neuron-specific *ank2*-RNA results in MB phenotypes similar to those seen in *Nrg* mutants (T.G. and P.C., unpublished).

MB lobe development, on the other hand, requires the NRG-180-specific intracellular fragment. We showed that PYD acts downstream of NRG-180 during the formation of α and β lobes. Consistent with this, we never observe axon stalling defects (i.e. lack of peduncle formation) in *pyd* mutants, whereas we do see defects in lobe outgrowth, branching and guidance. Furthermore, the neuron-specific NRG-180 isoform can bind directly to the first

PDZ-domain of this MAGUK protein. Our observation that NRG and PYD interact to mediate proper sister neurite projections defines a novel role for the ZO-1 homolog PYD in axonogenesis. Thus far, the best-known role of MAGUKs in the nervous system has been in synapse development and function, as is the case for one of the prototypic MAGUKs, *Drosophila Discs Large 1* (*Dlg1*) (Tejedor et al., 1997; Thomas et al., 1997), whereas PYD is known as a component of adherens junctions (Jung et al., 2006; Seppa et al., 2008).

Sema-1a, *trio* and *Rac1* were also found to be a part of the genetic network that interacts with *Nrg*. The observation that heterozygosity for mutations in *Sema-1a* and *trio* both suppress NRG-180 overexpression induced MB phenotypes indicates that *Sema-1a* and *trio* are genetically downstream of *Nrg* and possibly in the same pathway. By contrast, the introduction of a *Rac1* mutation in a *Nrg* gain- or loss-of-function background results in both cases in enhancement of MB phenotypes (see Fig. 7; see Table S2 in the supplementary material). This argues against a one-to-one signaling model between NRG and RAC1, in which RAC1 acts only downstream of NRG-180. Consistent with the genetic data, we could not detect a direct physical interaction between NRG-180 and RAC1 (data not shown), but preliminary co-immunoprecipitation data suggest that NRG-180 can bind to TRIO (Y.Y.K. and P.C., unpublished). Further experiments will be necessary to assess whether this binding also occurs in vivo, and whether it is instrumental for NRG-180-dependent modulation of RAC1 signaling.

Contrary to the observed genetic interaction between *Nrg* and *Sema-1a*, we found no evidence for interaction between *Nrg* and two genes that code for well-characterized Semaphorin receptors, *plexin A* and *plexin B* (data not shown). This is an unexpected observation in light of the fact that *Sema-1a* and *plexin A* and *plexin B* interact during mushroom body development (Liesbeth Zwarts, T.G. and P.C., unpublished). Therefore, this suggests that during mushroom body development Sema-1a acts both in a plexin-dependent and a plexin-independent way. A plexin-independent role in axon outgrowth has previously been described for vertebrate Sema7a (Pasterkamp et al., 2003).

The distinct requirement for NRG in peduncle and lobe formation is reminiscent of what has been shown for DSCAM. This protein has an early and essential role for selective fasciculation of young axons in the peduncle and is subsequently required for bifurcation and branch segregation (Wang et al., 2002; Zhan et al., 2004). In light of this, it is interesting to note that the different cell-adhesion molecules that have been implicated in MB development have a different MB expression pattern or temporal requirement for MB development. NRG is expressed in the MBs throughout its entire development, but we did not find any essential function for Neuroglian in larval MB development. By contrast, DSCAM expression disappears with fiber maturation and mutants have larval MB phenotypes (Zhan et al., 2004). Likewise, *Fas2* mutants display larval lobe defects, whereas no (Cheng et al., 2001; Kurusu et al., 2002) or almost no (Fushima and Tsujimura, 2007) lobe defects were found in adult mutants. Taken together, these observations suggest that different steps in MB axonogenesis depend on combinations not only of isoforms of the same cell-adhesion molecule (e.g. DSCAM) but also of different cell surface molecules (e.g. NRG, FAS2 and SEMA-1A). Jointly, the cell-surface molecule complement of any given axon combined with guidance signals will then control the signaling required for proper neural circuit formation in the MBs.

Acknowledgements

This work is supported by FWO grant G.0285.05 to P.C., and by grants from the NICHD (RO1HD29388) and the NSF (IBN-0132819) to M.H. We thank the following people for antibodies and fly stocks: Markus Affolter, Martin Heisenberg, Allen Spradling, Barry Dickson, Liqun Luo, Ryu Ueda, Joachim Schulz, Jennifer Zallen and Sean Sweeney. We are grateful to Mimi Deprez for help with preparing the manuscript and figures, and to Glen Legge for instructions on how to use the MolMol software. We acknowledge Carlos Dotti for critical reading of the manuscript. Deposited in PMC for release after 12 months.

Competing interests statement

The authors declare no competing financial interests.

Supplementary material

Supplementary material for this article is available at
http://dev.biologists.org/lookup/suppl/doi:10.1242/dev.052787/-/DC1

References

Adachi, Y., Hauck, B., Clements, J., Kawauchi, H., Kurusu, M., Totani, Y., Kang, Y. Y., Eggert, T., Walldorf, U., Furukubo-Tokunaga, K. et al. (2003). Conserved cis-regulatory modules mediate complex neural expression patterns of the eyeless gene in the Drosophila brain. *Mech. Dev.* **120**, 1113-1126.

Awasaki, T., Saito, M., Sone, M., Suzuki, E., Sakai, R., Ito, K. and Hama, C. (2000). The Drosophila trio plays an essential role in patterning of axons by regulating their directional extension. *Neuron* **26**, 119-131.

Bieber, A. J., Snow, P. M., Hortsch, M., Patel, N. H., Jacobs, J. R., Traquina, Z. R., Schilling, J. and Goodman, C. S. (1989). Drosophila neuroglian: a member of the immunoglobulin superfamily with extensive homology to the vertebrate neural adhesion molecule L1. *Cell* **59**, 447-460.

Brand, A. H. and Perrimon, N. (1993). Targeted gene expression as a means of altering cell fates and generating dominant phenotypes. *Development* **118**, 401-415.

Castellani, V., Chedotal, A., Schachner, M., Faivre-Sarrailh, C. and Rougon, G. (2000). Analysis of the L1-deficient mouse phenotype reveals cross-talk between Sema3A and L1 signaling pathways in axonal guidance. *Neuron* **27**, 237-249.

Castellani, V., De Angelis, E., Kenwrick, S. and Rougon, G. (2002). Cis and trans interactions of L1 with neuropilin-1 control axonal responses to semaphorin 3A. *EMBO J.* **21**, 6348-6357.

Cheng, Y., Endo, K., Wu, K., Rodan, A. R., Heberlein, U. and Davis, R. L. (2001). Drosophila fasciclinII is required for the formation of odor memories and for normal sensitivity to alcohol. *Cell* **105**, 757-768.

Clements, J., Hens, K., Francis, C., Schellens, A. and Callaerts, P. (2008). Conserved role for the Drosophila Pax6 homolog Eyeless in differentiation and function of insulin-producing neurons. *Proc. Natl. Acad. Sci. USA* **105**, 16183-16188.

Dahme, M., Bartsch, U., Martini, R., Anliker, B., Schachner, M. anad Mantei, N. (1997). Disruption of the mouse L1 gene leads to malformations of the nervous system. *Nat. Genet.* **17**, 346-349.

Davis, R. L. (2005). Olfactory memory formation in Drosophila: from molecular to systems neuroscience. *Annu. Rev. Neurosci.* **28**, 275-302.

Demyanenko, G. P., Tsai, A. Y. and Maness, P. F. (1999). Abnormalities in neuronal process extension, hippocampal development, and the ventricular system of L1 knockout mice. *J. Neurosci.* **19**, 4907-4920.

Dubreuil, R. R., MacVicar, G., Dissanayake, S., Liu, C., Homer, D. and Hortsch, M. (1996). Neuroglian-mediated cell adhesion induces assembly of the membrane skeleton at cell contact sites. *J. Cell Biol.* **133**, 647-655.

Fransen, E., Lemmon, V., Van Camp, G., Vits, L., Coucke, P. and Willems, P. J. (1995). CRASH syndrome: clinical spectrum of corpus callosum hypoplasia, retardation, adducted thumbs, spastic paraparesis and hydrocephalus due to mutations in one single gene, L1. *Eur. J. Hum. Genet.* **3**, 273-284.

Fransen, E., D'Hooge, R., Van Camp, G., Verhoye, M., Sijbers, J., Reyniers, E., Soriano, P., Kamiguchi, H., Willemsen, R., Koekkoek, S. K. et al. (1998). L1 knockout mice show dilated ventricles, vermis hypoplasia and impaired exploration patterns. *Hum. Mol. Genet.* **7**, 999-1009.

Fushima, K. and Tsujimura, H. (2007). Precise control of fasciclin II expression is required for adult mushroom body development in Drosophila. *Dev. Growth Differ.* **49**, 215-227.

Godenschwege, T. A. and Murphey, R. K. (2009). Genetic interaction of Neuroglian and Semaphorin1a during guidance and synapse formation. *J. Neurogenet.* **23**, 147-155.

Grootjans, J. J., Reekmans, G., Ceulemans, H. and David, G. (2000). Syntenin-syndecan binding requires syndecan-synteny and the co-operation of both PDZ domains of syntenin. *J. Biol. Chem.* **275**, 19933-19941.

Hakeda-Suzuki, S., Ng, J., Tzu, J., Dietzl, G., Sun, Y., Harms, M., Nardine, T., Luo, L. and Dickson, B. J. (2002). Rac function and regulation during Drosophila development. *Nature* **416**, 438-442.

Hall, S. G. and Bieber, A. J. (1997). Mutations in the Drosophila neuroglian cell adhesion molecule affect motor neuron pathfinding and peripheral nervous system patterning. *J. Neurobiol.* **32**, 325-340.
Hortsch, M. (2000). Structural and functional evolution of the L1 family: are four adhesion molecules better than one? *Mol. Cell. Neurosci.* **15**, 1-10.
Hortsch, M., Wang, Y. M., Marikar, Y. and Bieber, A. J. (1995). The cytoplasmic domain of the Drosophila cell adhesion molecule neuroglian is not essential for its homophilic adhesive properties in S2 cells. *J. Biol. Chem.* **270**, 18809-18817.
Hortsch, M., Homer, D., Malhotra, J. D., Chang, S., Frankel, J., Jefford, G. and Dubreuil, R. R. (1998a). Structural requirements for outside-in and inside-out signaling by Drosophila neuroglian, a member of the L1 family of cell adhesion molecules. *J. Cell Biol.* **142**, 251-261.
Hortsch, M., O'Shea, K. S., Zhao, G., Kim, F., Vallejo, Y. and Dubreuil, R. R. (1998b). A conserved role for L1 as a transmembrane link between neuronal adhesion and membrane cytoskeleton assembly. *Cell Adhes. Commun.* **5**, 61-73.
Huber, A. B., Kolodkin, A. L., Ginty, D. D. and Cloutier, J. F. (2003). Signaling at the growth cone: ligand-receptor complexes and the control of axon growth and guidance. *Annu. Rev. Neurosci.* **26**, 509-563.
Hung, A. Y. and Sheng, M. (2002). PDZ domains: structural modules for protein complex assembly. *J. Biol. Chem.* **277**, 5699-5702.
Islam, R., Kristiansen, L. V., Romani, S., Garcia-Alonso, L. and Hortsch, M. (2004). Activation of EGF receptor kinase by L1-mediated homophilic cell interactions. *Mol. Biol. Cell* **15**, 2003-2012.
Jung, A. C., Ribeiro, C., Michaut, L., Certa, U. and Affolter, M. (2006). Polychaetoid/ZO-1 is required for cell specification and rearrangement during Drosophila tracheal morphogenesis. *Curr. Biol.* **16**, 1224-1231.
Koradi, R., Billeter, M. and Wuthrich, K. (1996). MOLMOL: a program for display and analysis of macromolecular structures. *J. Mol. Graph.* **14**, 51-55, 29-32.
Koushika, S. P., Lisbin, M. J. and White, K. (1996). ELAV, a Drosophila neuron-specific protein, mediates the generation of an alternatively spliced neural protein isoform. *Curr. Biol.* **6**, 1634-1641.
Kurusu, M., Nagao, T., Walldorf, U., Flister, S., Gehring, W. J. and Furukubo-Tokunaga, K. (2000). Genetic control of development of the mushroom bodies, the associative learning centers in the Drosophila brain, by the eyeless, twin of eyeless, and Dachshund genes. *Proc. Natl. Acad. Sci. USA* **97**, 2140-2144.
Kurusu, M., Awasaki, T., Masuda-Nakagawa, L. M., Kawauchi, H., Ito, K. and Furukubo-Tokunaga, K. (2002). Embryonic and larval development of the Drosophila mushroom bodies: concentric layer subdivisions and the role of fasciclin II. *Development* **129**, 409-419.
Lee, T. and Luo, L. (1999). Mosaic analysis with a repressible cell marker for studies of gene function in neuronal morphogenesis. *Neuron* **22**, 451-461.
Lee, T., Lee, A. and Luo, L. (1999). Development of the Drosophila mushroom bodies: sequential generation of three distinct types of neurons from a neuroblast. *Development* **126**, 4065-4076.
Liu, L., Wolf, R., Ernst, R. and Heisenberg, M. (1999). Context generalization in Drosophila visual learning requires the mushroom bodies. *Nature* **400**, 753-756.
Maness, P. F. and Schachner, M. (2007). Neural recognition molecules of the immunoglobulin superfamily: signaling transducers of axon guidance and neuronal migration. *Nat. Neurosci.* **10**, 19-26.
Martini, S. R., Roman, G., Meuser, S., Mardon, G. and Davis, R.L. (2000). The retinal determination gene, dachshund, is required for mushroom body cell differentiation. *Development* **127**, 2663-2672.
Mehren, J. E., Ejima, A. and Griffith, L. C. (2004). Unconventional sex: fresh approaches to courtship learning. *Curr. Opin. Neurobiol.* **14**, 745-750.
Morin, X., Daneman, R., Zavortink, M. and Chia, W. (2001). A protein trap strategy to detect GFP-tagged proteins expressed from their endogenous loci in Drosophila. *Proc. Natl. Acad. Sci. USA* **98**, 15050-15055.
Ng, J., Nardine, T., Harms, M., Tzu, J., Goldstein, A., Sun, Y., Dietzl, G., Dickson, B. J. and Luo, L. (2002). Rac GTPases control axon growth, guidance and branching. *Nature* **416**, 442-447.
Noveen, A., Daniel, A. and Hartenstein, V. (2000). Early development of the Drosophila mushroom body: the roles of eyeless and dachshund. *Development* **127**, 3475-3488.
Pasterkamp, R. J., Peschon, J. J., Spriggs, M. K. and Kolodkin, A. L. (2003). Semaphorin 7A promotes axon outgrowth through integrins and MAPKs. *Nature* **424**, 398-405.
Seppa, M. J., Johnson, R. I., Bao, S. and Cagan, R. L. (2008). Polychaetoid controls patterning by modulating adhesion in the Drosophila pupal retina. *Dev. Biol.* **318**, 1-16.
Strauss, R. and Heisenberg, M. (1993). A higher control center of locomotor behavior in the Drosophila brain. *J. Neurosci.* **13**, 1852-1861.
Su, X. D., Gastinel, L. N., Vaughn, D. E., Faye, I., Poon, P. and Bjorkman, P. J. (1998). Crystal structure of hemolin: a horseshoe shape with implications for homophilic adhesion. *Science* **281**, 991-995.
Sun, S. C., Lindstrom, I., Boman, H. G., Faye, I. and Schmidt, O. (1990). Hemolin: an insect-immune protein belonging to the immunoglobulin superfamily. *Science* **250**, 1729-1732.
Sztriha, L., Frossard, P., Hofstra, R. M., Verlind, E. and Nork, M. (2000). Novel missense mutation in the L1 gene in a child with corpus callosum agenesis, retardation, adducted thumbs, spastic paraparesis, and hydrocephalus. *J. Child Neurol.* **15**, 239-243.
Tejedor, F. J., Bokhari, A., Rogero, O., Gorczyca, M., Zhang, J., Kim, E., Sheng, M. and Budnik, V. (1997). Essential role for dlg in synaptic clustering of Shaker K+ channels in vivo. *J. Neurosci.* **17**, 152-159.
Thomas, U., Kim, E., Kuhlendahl, S., Koh, Y. H., Gundelfinger, E. D., Sheng, M., Garner, C. C. and Budnik, V. (1997). Synaptic clustering of the cell adhesion molecule fasciclin II by discs-large and its role in the regulation of presynaptic structure. *Neuron* **19**, 787-799.
Wang, J., Zugates, C. T., Liang, I. H., Lee, C. H. and Lee, T. (2002). Drosophila Dscam is required for divergent segregation of sister branches and suppresses ectopic bifurcation of axons. *Neuron* **33**, 559-571.
Wang, X., Zhang, W., Cheever, T., Schwarz, V., Opperman, K., Hutter, H., Koepp, D. and Chen, L. (2008). The C. elegans L1CAM homologue LAD-2 functions as a coreceptor in MAB-20/Sema2 mediated axon guidance. *J. Cell Biol.* **180**, 233-246.
Xu, T. and Rubin, G. M. (1993). Analysis of genetic mosaics in developing and adult Drosophila tissues. *Development* **117**, 1223-1237.
Yamamoto, M., Ueda, R., Takahashi, K., Saigo, K. and Uemura, T. (2006). Control of axonal sprouting and dendrite branching by the Nrg-Ank complex at the neuron-glia interface. *Curr. Biol.* **16**, 1678-1683.
Yu, H. H., Araj, H. H., Ralls, S. A. and Kolodkin, A. L. (1998). The transmembrane Semaphorin Sema is required in Drosophila for embryonic motor and CNS axon guidance. *Neuron* **20**, 207-220.
Zhan, X. L., Clemens, J. C., Neves, G., Hattori, D., Flanagan, J. J., Hummel, T., Vasconcelos, M. L., Chess, A. and Zipursky, S. L. (2004). Analysis of Dscam diversity in regulating axon guidance in Drosophila mushroom bodies. *Neuron* **43**, 673-686.
Zhao, X. and Siu, C. H. (1996). Differential effects of two hydrocephalus/MASA syndrome-related mutations on the homophilic binding and neuritogenic activities of the cell adhesion molecule L1. *J. Biol. Chem.* **271**, 6563-6566.